RESULTS FROM THE SLAC NLC TEST ACCELERATOR[1]

R. D. Ruth, C. Adolphsen, S. Allison, R. Atkinson, W. Baumgartner, P. Bong, V. Brown, M. Browne, G. Caryotakis, R. Cassel, G. Cisneros, S. L. Clark, T. Constant, C. Corvin, T. Dean, J. Eichner, R. Fowkes, R. Fuller, S. Gold, J. Grippe, S. Hanna, H. Hoag, P. Holik, S. Holmes, R. Humphrey, L. Johnson, R. Jones, E. Jongewaard, K Ko, R. Koontz, N. Kroll, T.Lavine, G. A. Loew, R. Loewen, R. H. Miller, J. Minister, V. Nesterov, C. Nantista, J. M. Paterson, C. Pearson, R. Phillips, M. Pietryka, R. Pope, T. Porter, J. Rifkin, W. Roster, M. Seidel, H. Smith, S. Smith, J. Spencer, N. Spencer, D. Sprehn, S. Tantawi, P. Tenenbaum, A. Tillghman, A. Vlieks, V. Vylet, J. W. Wang, P. B. Wilson, Z. Wilson, E. Wright, D. Yeremian, J. Zelinski, C. Ziomek
Stanford Linear Accelerator Center, Stanford, CA 94309

Abstract

The design for the Next Linear Collider (NLC) at SLAC is based on two 11.4 GHz linacs operating at an unloaded acceleration gradient of 50 MV/m increasing to 85 MV/m as the energy is increased from 1/2 TeV to 1 TeV in the center of mass[1]. During the past several years there has been tremendous progress on the development of 11.4 GHz (X-band) RF systems. These developments include klystrons which operate at the required power and pulse length, pulse compression systems that achieve a factor of four power multiplication and structures that are specially designed to reduce long-range wakefields. Together with these developments, we have constructed a 1/2 GeV test accelerator, the NLC Test Accelerator (NLCTA)[2]. The NLCTA will serve as a test bed as the design of the NLC is refined. In addition to testing the RF system, the NLCTA is designed to address many questions related to the dynamics of the beam during acceleration, in particular, multibunch beam-loading compensation and transverse beam break-up. In this paper we describe the NLCTA and present results from initial experiments.

1 INTRODUCTION

The Next Linear Collider Test Accelerator (NLCTA) is a 42-meter-long beam line consisting consecutively, of an injector, a chicane, a linac, and a spectrometer.

The injector is a 150-KeV gridded thermionic-cathode gun, an X-band prebuncher, a capture section, and a preacceleration section. Downstream from the injector we have a magnetic chicane for longitudinal phase-space manipulation, energy measurement and collimation. After the collimation, the average current injected into the linac is comparable to the NLC specification, 1.0 ncoul/1.4 ns.

The NLCTA linac consists of up to six 1.8-meter-long X-band accelerator sections which are designed to suppress the long-range transverse wakefield. These sections are powered by three 50-MW klystrons whose peak power is quadrupled by SLED-II rf pulse compressors. This yields an unloaded acceleration gradient of 50 MV/m so that the maximum energy gain of the beam in the linac is 540 MeV. The NLCTA RF system parameters are listed in Table 1.

Downstream from the linac we have a magnetic spectrometer that can analyze the bunch train after acceleration. A vertical kicker magnet in the spectrometer provides a method for separating the bunches vertically so that the energy and energy spread can be measured along the bunch train. We can also measure the emittance in the spectrometer and in the chicane.

Table 1. NLCTA RF System Parameters

Parameter	Design	Upgrade
Linac Energy	540 MeV	920 MeV
Active Length	10.8 m	10.8m
Acc. Gradient	50 MeV	85 MeV
Inj. Energy	90 MeV	90 MeV
RF Freq.	11.4 GHz	11.4 GHz
No. of Klystrons	4	7
Klystron Power	50 MW	75 MW
Klystron Pulse	1.5 μsec	1.5 μsec
RF Compression	4.0	4.0
Structure Length	1.8 m	1.8 m

In the next few sections we present an overview of the NLCTA, and we conclude the paper with a discussion of results from initial experiments.

2 CONVENTIONAL SYSTEMS

All the conventional systems for the NLCTA are complete. All of the non-RF components in the beam line are installed; this includes magnets, beam position monitors, vacuum system and all shielding and cabling. All of the power supplies are installed and tested and are operated routinely with the NLCTA control system which is an extension of the SLC control system. The thermionic electron gun and all injector solenoids are installed and tested. Presently, the beam line is under vacuum with the two injector structures installed and two of the six linac accelerator structures installed.

[1] Work supported by Department of Energy contract DE-AC03-76SF00515.

0-7803-4376-X/98/$10.00 © 1998 IEEE

3 THE RF SYSTEM

A schematic layout of the NLCTA RF system is shown in Fig. 1. The beam is initially bunched with two pre-buncher cavities at the fundamental frequency of 11.424 GHz. It is then accelerated in two 0.9 m-long RF structures with an unloaded energy gain of 90 MeV. The first of these two injector structures has several low-beta cells to capture the beam optimally. The injector accelerators and prebunchers are powered by a single 50 MW klystron compressed by a factor of 4 by a SLED-II pulse compression system. After the chicane, the linac consists of six 1.8 m-long structures (two presently installed). Each of the first two pairs is powered by a single 50 MW klystron. The final pair of structures and final klystron will use the SLED-II compression system in common with the middle pair of the linac.

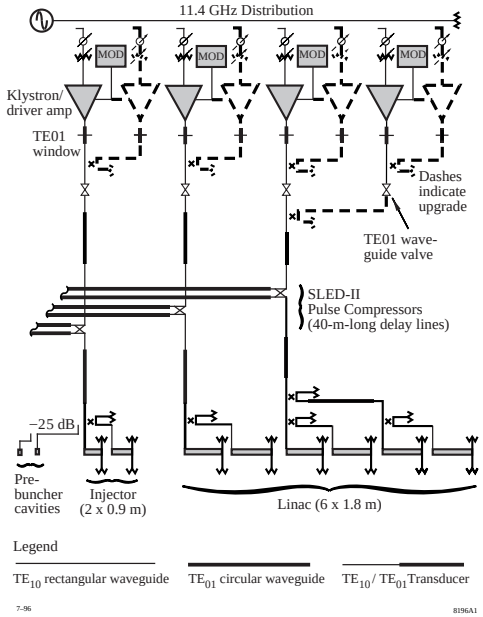

Figure 1. A schematic of the NLCTA rf system

4 KLYSTRONS

The NLCTA (and NLC) specifications call for a 50 MW Klystron operating with a 1.5 μsec pulse length (1.2 μsec for the NLC). Thus far the klystron development effort at SLAC has produced five klystrons that meet or exceed the NLCTA specification [3]. In Fig. 2 you see the output power of the fourth in the series, XL-4. It is a very robust klystron with a very stable output power. As you can see from Fig. 2, XL-4 can produce a 75 MW pulse 1.2 μsec long. Both XL-2 and XL-3 also produce more than the required 50 MW and all of the three klystrons have the required bandwidth to work with the SLED-II compression system. The first XL-4 klystron has been installed on the NLCTA injector modulator and is being used to power the injector of the NLCTA. The second XL-4 klystron has been installed in the first RF station of the NLCTA linac and is presently being used to power the first two accelerator structures of the linac.

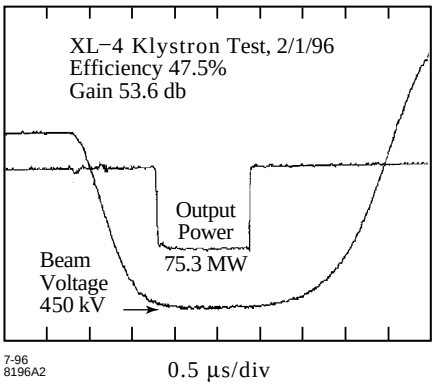

Figure 2. High-Power test of XL-4.

Several more klystrons of the XL-4 type will be produced for the NLCTA. However, the development effort for NLC klystrons has been turned towards the development of a periodic permanent magnet (PPM) focused klystron[4]. This eliminates the focusing solenoid from the klystron which reduces both the capital and operating cost significantly. The initial tests of the first PPM klystron have yielded up to 60 MW with about 60% efficiency. This klystron power exceeds the 50 MW required for the 0.5 TeV NLC.

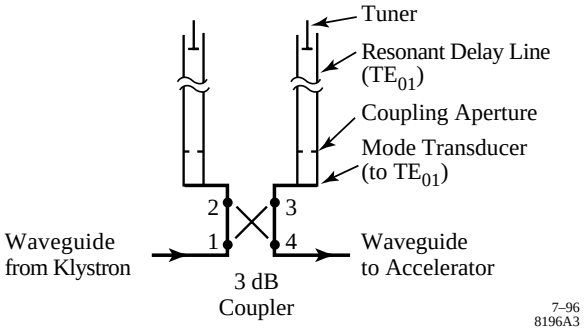

Figure 3. A schematic of the SLED-II rf compression.

5 RF PULSE COMPRESSION

A schematic diagram of the SLED-II compression system is shown in Fig. 3. The klystron power flows through a 3-dB hybrid where it is split to resonantly charge two delay lines. After several round trip times the klystron phase is flipped by 180 degrees, after which the power from the klystron adds to the power emitted from the delay lines to create a compressed pulse of RF power.

In Fig. 4 you see the results of low power and high power tests of the injector SLED-II. The cold tests show the expected pulse compression of four, and the high-power tests follow the cold tests quite closely.

All three SLED-II systems have been installed in the NLCTA, and the injector compression system and the first linac compresion system have been conditioned up to about 180 MW output. The tests of the these two SLED-II systems have shown excellent performance with an overall efficiency that exceeded our expectations.

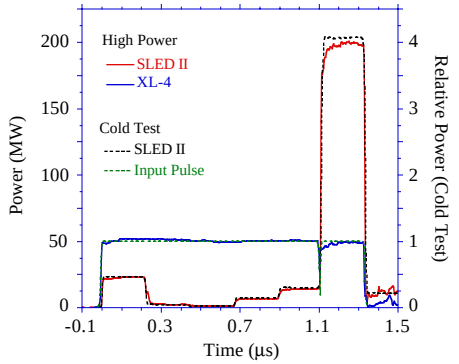

Figure 4. Test of Injector SLED-II system.

6 RF STRUCTURES

The NLC requires accelerator structures that operate reliably with an unloaded gradient of 50 MV/m for the 0.5 TeV collider and 85 MV/m for the 1.0 TeV upgrade. The NLCTA will serve as a model of this upgrade path in that we will begin at the lower acceleration gradient and eventually increase the gradient to the required 85 MV/m (see Table 1).

In addition to the gradient requirement, the NLC structures must be designed to substantially reduce the long-range transverse wakefields that can cause beam breakup. To achieve this reduction we have pursued two basic types of accelerator structures, the detuned structure and the damped-detuned structure. As you can see in Fig. 1, there are a total of eight structures in the NLCTA. The first two are one-half-length detuned structures. The second pair are full-length detuned structures. The third pair are damped-detuned structures; and finally, the last pair will be damped-detuned structures.

6.1 Detuned Structures

In a constant gradient traveling wave structure the irises are tapered to vary the group velocity in order to keep the gradient constant in spite of the loses in the structure. This tapering produces a variation of the frequency of the first dipole mode along the structure length that can be as much as 10%. The detuned structure takes advantage of this by changing the profile of the iris taper in order to create a smooth Gaussian-like distribution of higher-order modes. This leads to a Gaussian like initial decay of the wake field behind the bunch[7]. We have succesfully tested this concept using probe and witness beams in the Accelerator Structure Test Set-up (ASSET) facility in the SLC[8]. There are four detuned structures in the NLCTA.

6.2 High-Power Tests of Structures

During the past several years we have performed many high-power tests of different types of structures[9]. These tests indicate that surface fields up to 500 MV/m can be obtained in copper structures at 11.4 GHz. In power-limited tests, average acceleration gradients in short structures have reached 120 MV/m[10]. The first 1.8 m detuned structure has been high-power tested up to 67 MV/m[11]. Thus far, the injector sections in the NLCTA have been conditioned up to 55 MV/m average accelerating gradient while the first two linac structures have been conditioned up to 45 MV/m.

6.2 Damped-Detuned Structures

In order to further reduce the wakefield and the tolerances, it is necessary to provide some moderate damping for the higher-order dipole modes. To accomplish this we have developed a damped-detuned structure that uses four symmetrically placed manifolds to provide the damping [12]. A schematic of the cell for the structure is shown in Fig. 5. The structure cells are coupled to four waveguides that are formed when the cells are diffusion bonded together. The dipole mode is coupled out to the waveguide where is propagates to the end of the structure to a load. This technique damps the first dipole modes with Qs of about 1000. The signals from the manifold can be used as a beam position monitor to align the structure to the beam.

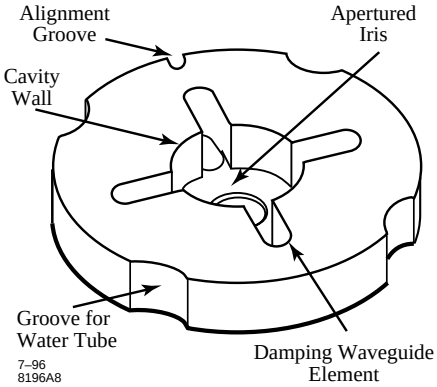

Figure 5. A cell of the Damped-Detuned structure.

The first two damped-detuned structures have been constructed in collaboration with KEK[13,14]. The first of these, DDS1, has been tested in the ASSET facility. The results of the experiment are shown in Fig. 6. The measured long-range transverse wakefield is reduced by more than two orders of magnitude realtive to the short-range wake and agrees well with the theoretical predictions[14,15]. Finally, the modes that are damped have now been shown to yield a sensitive position measurement along the length of the structure[16].

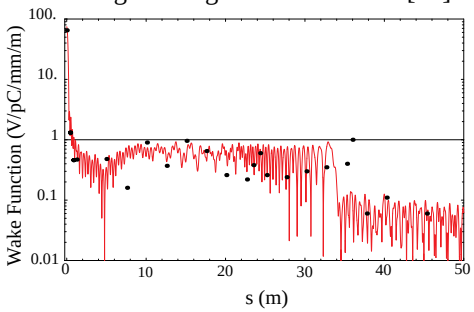

Figure 6. Tests of the Damped-Detuned structure. Points are data while the curve is a theoretical prediction.

7 BEAM LOADING EXPERIMENTS

Presently, we are accelerating beam up to 60 MV in the NLCTA injector and an additional 140 MV in the two installed structures of the NLCTA linac. This yeilds 200 MV in the spectrometer.

The first round of experiments in the NLCTA address the primary goal for beam dynamics studies: to acieve an rms energy spread of 10^{-3} with the NLC beam loading. To accomplish this it is nessesary to tailor the RF pulse for one filling time so that it matches the steady state beam loaded profile for the desired current. All subsequent bunches then serve to keep the beam in the steady state.

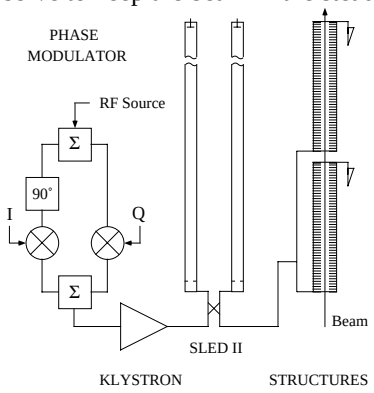

Figure 7. Layout of an RF station including the phase modulator which is controlled by the I & Q inputs.

This profile is closely matched by a simple ramp of the RF amplitude in the output from the SLED-II compression system. To achieve this ramp in the NLCTA we take advantage of the addition of several time bins of RF in the SLED system. By varying the phase in a programmed manner, the resultant RF output from SLED-II can be a linear ramp, or any variation thereof.

A conceptual diagram of the fast phase variation system is shown in Fig. 7. The phase modulator is controlled by I and Q modulators driven by an arbitrary function generator. The phase programming chosen for this experiment is shown in Fig. 8. You see that the resulting ramp of the RF amplitude in the compressed pulse is quite linear.

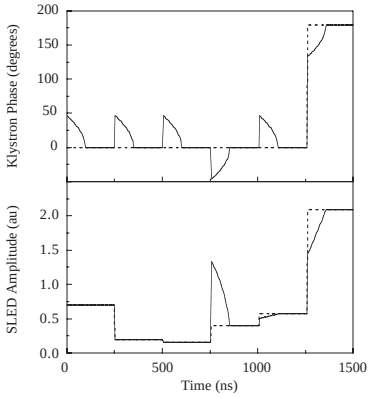

Figure 8. Phase profile (upper plot) of the klystron RF drive and resulting SLED output amplitude (lower plot) for 13% loading (solid line) and no loading (dashed).

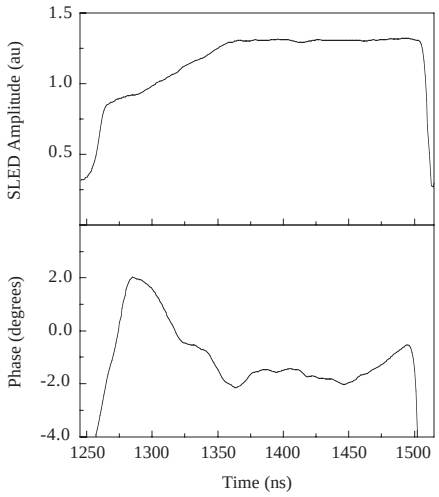

Figure 9. Measured RF amplitude (top plot) and phase (bottom plot) out of SLED when the klystron drive was phased to compensate 13% beam loading.

The measured RF output from the linac SLED-II system is shown in Fig. 9. The amplitude is quite linear while the phase changes over the ramp are about 4 degrees.

In order to measure the effect of this RF profile on the accelerated beam the NLCTA has been equipped with a kicker magnet upstream of the spectrometer magnet which provides a dipole field that ramps linearly in time during the 120 ns bunch train passage. In the plane of the spectrometer profile monitor, the vertical direction is mapped to position within the bunch train while the horizontal position is mapped to the beam energy.

In Fig. 10 you see two cases, one for uncompensated beam loading and one for compensated beam loading. In the uncompensated case, there is a large transient due to the beam loading after which in the upper part of the figure the beam reaches steady state. In the compensated case the transient has been completely compensated yielding a 200 MeV beam with 1/3 A current with a full spread of about 0.3% in relative energy. Therefore, with 1/2 the desired average current for the NLC, it seems to be quite straightforward to compensate all beam loading effects locally along the length of the linac.

.

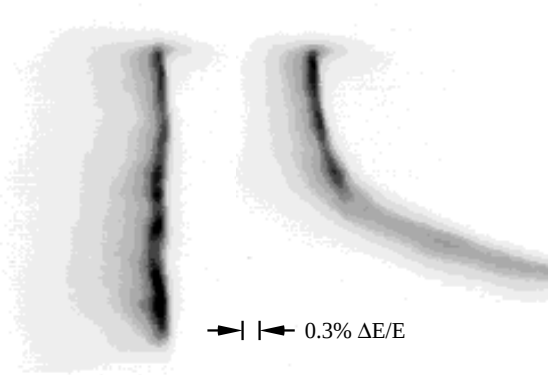

Figure 10. Profile monitor images of the bunch train at the end of the spectrometer.

The kicker magnet has spread the 120 ns train length vertically with head of the train at the bottom. The dispersion generated by the spectrometer bend magnet has spread the electrons horizontally in proportion to their energy with higher energy toward the right. The left image was recorded with 13% loading compensation in the linac and right image with no linac compensation.

9 ACKNOWLEDGMENTS

The installation of the accelerator structures, modulator, and klystron for the third RF station in the NLCTA is taking place during this conference. This marks the end of the NLCTA project, and the beginning of an active experimental program for the NLC. We would like to thank the SLAC Technical Division Directorate and Department Heads for their support during construction and commsioning of the NLCTA.

REFERENCES

[1] Zeroth-Order Design Report for the Next Linear Collider, SLAC Report 474, 1996.

[2] R. D. Ruth *et al*., "The Next Linear Collider Test Accelerator", SLAC-PUB-6293, in Proc. 1993 Part. Accel. Conf., Washington, DC, 543-545 (1993).

[3] G. Caryotakis, "The X-Band Klystron Development Program at SLAC", SLAC-PUB-7146, in Proc. of the 3rd Int. Wksp. on Pulsed RF Sources for Linear Colliders, Hayama, Japan, 1996.

[4] D. Sprehn *et al.*, "PPM Focused X-Band Klystron Development at SLAC", SLAC-PUB-7231, in Proc. of the 3rd Int. Wksp. on Pulsed RF Sources for Linear Colliders, Hayama, Japan, 1996.

[5] S. G. Tantawi *et al*., "Performance Measurements of SLAC's X-band High-Power Pulse Compression System (SLED-II)", SLAC-PUB-6775, submitted for publication.

[6] S. G. Tantawi, *et al*., "The Next Linear Collider Test Accelerator's RF Pulse Compression and Transmission Systems", Proc. of EPAC96, Sitges, Spain and in SLAC-PUB-7247.

[7] K. L. F. Bane and R. L. Gluckstern, "The Transverse Wakefield of a Detuned X-Band Accelerating Structure", SLAC-PUB-5783, Part. Acc. **42**, 123 (1993).

[8] C. Adolphsen *et al*., "Measurement of Wakefield Suppression in a Detuned X-Band Accelerator Structure", SLAC-PUB-6629, Phys. Rev. Lett. **74**: 1759-1762 (1995).

[9] J. W. Wang *et al*., "High-Gradient Tests of SLAC Linear Collider Accelerator Structures", SLAC-PUB-6617, Proc. of the 1994 Int. Linac Conf., Tsukuba, Japan, 305-307 (1994).

[10] J. W. Wang *et al*., "SLAC/CERN High-Gradient Tests of an X-band Accelerating Section", CERN-SL-95-27-RF, SLAC-PUB-6617, in Proc. of 16th IEEE Part. Acc. Conf., Dallas Texas, 1995.

[11] S. Takeda *et al*., "High Gradient Experiments by the ATF", Proc. of the 1991 Part. Acc. Conf., San Francisco, CA, 2061-2063 (1991).

[12] R. M. Jones *et al*., "Equivalent Circuit Analysis of the SLAC Damped Detuned Structure", Proc. of EPAC96, Sitges, Spain and in SLAC-PUB-7187..

[13] R. H. Miller *et al.*, "A Damped Detuned Structure for the Next Linear Collider", Proc. of LINAC96, Geneva, Switzerland.

[14] R. M. Jones *et al.*, "A Spectral Method Applied to the Calculation of the Wake Function for the NLCTA", Proc. of LINAC96, Geneva, Switzerland.

[15] C. Adolphsen *et al.*, submitted for publication.

[16] M. Seidel *et al.*, "Microwave Analysis of the Damped Detuned Accelerator Structures", Proc. of LINAC96, Geneva, Switzerland.